



Cite this: *Mater. Adv.*, 2023,  
4, 5753

# Flexible, antibacterial porous phase change thermal management film prepared by a one-step extrusion casting-foaming method†

Xinyu Guo,<sup>a</sup> Tianyu Xing,<sup>a</sup> Yanqin Huang<sup>a</sup> and Jiachun Feng \*<sup>ab</sup>

Flexible antibacterial thermal management products with long working duration are highly desirable for personalized healthcare applications, such as thermotherapy. However, the preparation of products that can meet all these requirements is still under development. In this study, we prepared a flexible porous phase change foaming film (PCFF) by a facile one-step extrusion casting-foaming method, in which thermal expansion microspheres (EMs) were used as the foaming agent to foam a poly(styrene-*b*-(ethylene-co-butylene)-*b*-styrene (SEBS)/paraffin-based phase change system containing an antibacterial agent-grafted functional polypropylene (ab-PP) masterbatch. The addition of the ab-PP masterbatch not only improved the processability of the blend system but also imparted the PCFF with almost 100% antibacterial rate against both *Escherichia coli* and *Staphylococcus aureus*. The phase change of paraffin and presence of abundant pores within the resulting foaming film bestowed the PCFF with excellent long-duration temperature stability. For a stack composed of 5 layers PCFFs with a total thickness of 3.7 mm and mass of only 16.2 g, the duration of temperature decrease from 48 to 35 °C (simulating the thermotherapy temperature for the human body) is longer than 10 minutes. The resultant PCFF exhibited excellent flexibility, antibacterial performance and exothermic ability, which made it a promising prospect in wearable thermotherapy fields.

Received 9th August 2023,  
Accepted 14th October 2023

DOI: 10.1039/d3ma00524k

rsc.li/materials-advances

## Introduction

With the enhancement of health awareness, there is a growing demand for thermal management products that possess excellent flexible and antibacterial properties, as well as long-term working duration.<sup>1–4</sup> Among the various thermal management materials, phase change materials (PCMs) have garnered extensive attention due to their thermostatic exothermic ability in the process of phase change. Paraffin is one of the most representative PCMs, owing to the advantages of high phase change enthalpy, low subcooling degree, rich variety, environmental friendliness and low price.<sup>5,6</sup> However, similar to the other PCMs, when the external heat input surpasses the maximum enthalpy value of paraffin, it undergoes heating or cooling through the sensible

heat method, resulting in a short work duration when used in personalized healthcare applications, such as thermotherapy treatment.<sup>7–9</sup> To overcome this challenge and achieve long-term work ability, various approaches have been explored to extend the phase change duration of PCMs. Among these approaches, incorporating PCMs with porous materials to prepare low-thermal conductivity (TC) materials has been proven to be an effective method.<sup>10,11</sup> The existence of multiple air pores, which have a TC as low as 0.0267 W m<sup>−1</sup> K<sup>−1</sup>, can slow down the heat transfer rate, thereby prolonging the exothermic process of PCMs and achieving a longer-duration thermotherapy.<sup>12</sup> Up to now, the preparation of porous phase change systems by absorbing the melted paraffin into porous skeletons, including various aerogels,<sup>13</sup> sponges<sup>14</sup> and foams,<sup>15</sup> has been widely reported. However, this adsorption approach, involving the preparation of suitable porous frameworks and subsequent melted paraffin absorption, has some disadvantages. Besides the time-consuming and energy-consuming operations, the size and performance of the resultant porous phase change composite materials are strongly limited by the characteristics of the skeleton material. The intrinsic brittleness and fragility of these porous skeletons make it difficult to flexibly prepare porous PCMs with good mechanical properties, large deformation ability and arbitrary size, which are highly required characteristics for wearable application.<sup>16</sup>

<sup>a</sup> State Key Laboratory of Molecular Engineering of Polymers, Department of Macromolecular Science, Fudan University, Shanghai 200433, China.  
E-mail: jcfeng@fudan.edu.cn

<sup>b</sup> Yiwu Research Institute of Fudan University, Yiwu City, Zhejiang 322000, China

† Electronic supplementary information (ESI) available: SEM micrographs of the as-received EMs, expanded EMs. Infrared spectra and GPC result of ab-PP masterbatch. Density, porosity, and diameter distribution histograms of SPWT and SPWTPP. Schematic diagrams of the SPWPP film structure at high temperature and room temperature. Elastic modulus of SPW, SPWPP, SPWT and SPWTPP. See DOI: <https://doi.org/10.1039/d3ma00524k>

To overcome these limitations, research studies have attempted to directly introduce pores into PCMs by foaming them to prepare a porous phase change system. However, molten PCMs typically have very low strength to stabilize pores, which make directly foaming very difficult. By blending PCMs with linear low-density polyethylene (LLDPE) and further crosslinking, Sobolciak *et al.*<sup>17</sup> once foamed a paraffin-containing system using a chemical blowing agent, obtaining a porous LLDPE/paraffin phase change foaming material. Unfortunately, the paraffin content was only 30 wt% due to the low melt strength, which resulted in a low phase change enthalpy of 22.4–25.1 J g<sup>-1</sup>. More recently, we demonstrated a facile method for foaming a poly(styrene-*b*-(ethylene-*co*-butylene)-*b*-styrene (SEBS)/paraffin phase change system using thermal expansion microspheres (EMs) as the foaming agent. This approach involved hot press-foaming after mixing all components in a cyclohexane solvent and drying.<sup>18</sup> Owing to the excellent mechanical properties of SEBS and its encapsulation capacity for paraffin derived from the mid-block selectivity to paraffin, the resulting porous phase change system possessed high enthalpy value and good flexibility. However, this method involved the use of the organic solvent and non-continuous mould-foaming technology, so it still remains a challenge for the large-scale fabrication of flexible thermal management materials with long work duration through a green process method.

In addition to flexibility and long-term performance, achieving antibacterial properties is another crucial aspect in personalized healthcare applications including thermotherapy treatment. Antibacterial properties can be endowed by introducing components with antibacterial function<sup>19</sup> *via* physically blending with the system or chemically attaching to the molecular chains of the material. Physically blending has the advantage of convenient operation, but it may easily migrate to the surface of the material, resulting in poor performance during practical use. Alternatively, chemically attaching antibacterial agents to the material's molecular chains can provide a permanent antibacterial property, and is thus more suitable for the wearable applications. Zheng *et al.*<sup>20</sup> prepared an antibacterial agent-grafted functionalized polypropylene masterbatch (ab-PP) with long-term antibacterial properties by a melting reaction of polypropylene-*graft*-maleic anhydride with polyhexamethylene guanidine hydrochloride oligomer. They further used the ab-PP masterbatch to melt-blend with polyethylene terephthalate, preparing a polymer blend that possessed the antibacterial rate of above 98.0% against both *Escherichia coli* (*E. coli*) and *Staphylococcus aureus* (*S. aureus*).<sup>21</sup>

Polypropylene (PP) is an important general polymer material. The excellent comprehensive properties, low price, nontoxicity, tasteless, hygienic safety, chemical stability and other properties make it an ideal material for medical and healthcare applications. PP is frequently blended with SEBS and mineral oil to prepare thermoplastic elastomer materials with exceptional properties such as elasticity, softness, and weather resistance.<sup>22,23</sup> It was found that the introduction of PP can largely improve the hardness, mechanical strength and melt processability of SEBS/mineral oil systems. Inspired by these findings, incorporating the antibacterial agent-grafted PP with the SEBS/paraffin/EMs system is not only expected to endow the phase change

system with antibacterial properties, but also may improve its melt processability.

In this work, we attempted to prepare paraffin-based porous phase change foaming materials *via* a facile one-step extrusion casting method, in which SEBS was used as the supporting material for paraffin, EMs was used as the foaming agent, and ab-PP masterbatch was employed to endow the blend system with excellent antibacterial ability and improved melt processability. By optimizing the premixing method and extrusion casting processing conditions, abundant pores were introduced into the SEBS/paraffin/ab-PP blend and the resulting flexible phase change foaming film (PCFF) exhibited outstanding antibacterial properties and long thermal management duration. The heat charge and heat release results suggested that the PCFF had fast heat-charging and slow heat-release characteristics, making it an ideal candidate for personalized healthcare applications. In view of these advantages, we used PCFF to make various thermotherapy products such as eye-shades, knee pads, and other products for multiple human body parts. The results indicated that these products showed good long-duration thermotherapy effect, which makes our materials have great potential for application in the wearable healthcare field.

## Experimental section

### Materials

Cyclohexane and paraffin with a melting temperature of  $T_m = 52\text{ }^{\circ}\text{C}$  (PW) were purchased from Sinopharm Chemical Reagent Company (Shanghai, China). SEBS triblock copolymer (Kraton G1654) was the product of Kraton Polymers, Inc. According to the manufacturer's instructions, the mass ratio of the PS and PEB block was 31:69. The molecular weight ( $M_w$ ) measured by GPC was  $1.88 \times 10^5\text{ g mol}^{-1}$  and the polydispersity index was 1.19.

The thermal expansion microspheres (EMs, Clozell 180DU45) were the product of PolyChem Alloy (USA). According to the technical data sheet, EMs were composed of the polyacrylonitrile (PAN) shell and the hydrocarbon gas filled in the shell. When the temperature was 120–129  $^{\circ}\text{C}$ , the thermoplastic shell began to soften, the internal hydrocarbons vaporized into gas and the volume of the microspheres gradually increased. When the temperature reached 175–185  $^{\circ}\text{C}$ , the volume of the microspheres expanded to the maximum without collapse. After cooling, the PAN shell solidified and the expanded shape was maintained. Scanning electron microscopy micrographs of the as-received EMs and expanded EMs in air were shown in Fig. S1 (ESI†).

The ab-PP masterbatch, prepared by a melting reaction of polypropylene-*graft*-maleic anhydride with polyhexamethylene guanidine hydrochloride oligomer (PHMG), was purchased from Shanghai Fuyuan Plastic Technology Co., Ltd (Shanghai, China). According to the information provided by the merchant, the content of the guanidinium oligomer is less than 20 wt%. The antimicrobial mechanism of PHMG is generally believed to destroy the membrane of the bacterial cells, and cause the leakage of the intracellular contents and the death of bacteria.<sup>20,21</sup> The absorption peaks at 3175  $\text{cm}^{-1}$  and 1636  $\text{cm}^{-1}$  in the infrared spectrum (Fig. S2, ESI†) of the ab-PP correspond to the stretching



vibration peaks of N–H and guanidine group, respectively, which further proved the successful grafting of the guanidine group. The  $M_w$  of ab-PP masterbatch determined by GPC (Fig. S3, ESI†) was  $2.1 \times 10^5 \text{ g mol}^{-1}$ .

### Preparation of the porous phase change foaming films

The preparation of PCFF consisted of two steps: Firstly, prepared the premix. We froze the paraffin slices with liquid nitrogen, and then grounded the paraffin into powder in a mechanical pulverizer. The ab-PP was also grounded into powder through similar freezing and pulverizing steps. Next, we weighed the paraffin powder, SEBS, EMs and ab-PP powder according to a set mass ratio (SEBS:paraffin:PP:EMs = 20:65:5:10) and physically mixed them to obtain a premix for extrusion casting. Secondly, fabricated the PCFF. PCFF were prepared by extrusion casting using a HAAKE single-screw extruder (length to diameter ratio 25:1) equipped with a T-shaped die (length  $\times$  width = 10  $\times$  1 mm). The melt processing temperatures of each section were 140, 180, 170 and 165 °C, and the speed of the screw was 40 rpm. The obtained PCFF was denoted as SPWTTP, in which S, PW, T, and PP represented SEBS, paraffin, EMs, and ab-PP masterbatch, respectively. For comparison, SEBS/paraffin phase change film (SPW, without EMs and ab-PP masterbatch), SEBS/paraffin/PP phase change film (SPWPP, with ab-PP masterbatch and without EMs), and SEBS/paraffin/EMs PCFF (SPWT, with EMs and without ab-PP masterbatch) were each prepared.

### Characterization

**Morphological observation.** The scanning electron microscope images were taken on an Ultra 55 field emission scanning electron microscope (FESEM, Zeiss, Germany) at an accelerating voltage of 3 kV. All of the fracture surfaces of samples were sputtered with a thin layer of gold before observation.

**Mechanical properties measurements.** An Instron 5966 universal testing machine (Instron, USA) was used to test the mechanical properties of the foaming samples.

**Differential scanning calorimetry (DSC).** Data of thermal energy storage and release properties were collected by Q2000 differential scanning calorimetry (TA, USA) instrument with a scan rate of 10 °C min<sup>−1</sup> under N<sub>2</sub> environment.

**Density measurements.** A densimeter was utilized to test the densities of all foamed and unfoamed samples at 25 °C.

**Rheological performance test.** The storage modulus ( $G'$ ), loss modulus ( $G''$ ) and viscosity of the material as a function of frequency were tested by a rotational rheometer (ThermoFisher, USA).

**Contact angles.** Contact angles were measured using a JC2000DM contact angle instrument (Zhongchen Digital Testers Co., Ltd, Shanghai, China) by the Sessile drop method using water (Milli-Q).

**Leakage test.** Firstly, samples were placed in a watch glass with a filter paper, and then the watch glass was placed in an oven at 80 °C. During the test duration of 10 min, the leakage of the sample was observed.

**Antibacterial test.** The antibacterial test method of samples against *E. coli* and *S. aureus* involved the plate spread count method. Firstly, the bacterial solution was diluted to 10<sup>6</sup> CFU mL<sup>−1</sup>, then 200  $\mu$ L of the diluted bacterial solution was dropped on the sample surface, and it was then covered with a covering film. No sample was added to the control group. The above samples were placed in a 37 °C constant-temperature incubator and incubated for 24 h. After the culture completed, they were rinsed with 20 mL of sterile phosphate buffer saline (PBS). The bacterial solution was serially diluted 10 times with sterile PBS solution, and 100  $\mu$ L of the diluted solution was evenly distributed on the LB solid medium. Then, they were placed in a 37 °C constant-temperature incubator for 18 h. After that, the samples were taken out and photographs were taken to record the number of colonies.

**Thermotherapy performance test.** PCFF was combined with textiles to prepare thermotherapy products, such as knee pads. The kneepad was wrapped around the knee, then wrapped in cotton cloth. A thermocouple was inserted into the kneepad, and the temperature change was recorded during the cooling process of the kneepad. Infrared images were recorded by a FLIR ONE PRO Thermal Imager (Pumeng Optoelectronics Technology Co., Ltd, Shanghai, China). All participant experiments including shape memory property and thermotherapy performance demonstration were standardized with the informed consent of the volunteers, and approved by the Institutional Review Board at Fudan University.

## Results and discussion

### Preparation and properties of SPWTTP PCFF

As illustrated in Fig. 1, our preparation process of PCFF consists of two steps: (1) preparing premix; (2) extrusion casting-

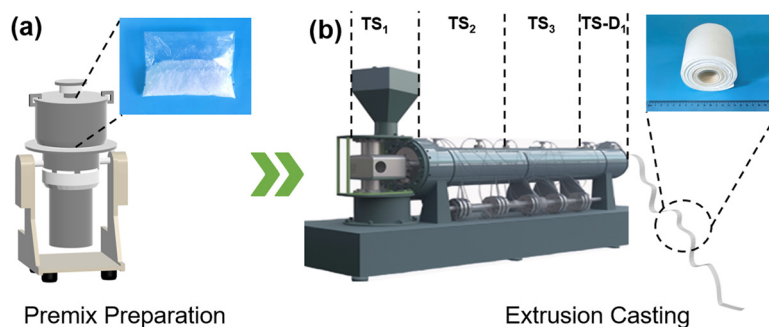


Fig. 1 (a) Schematic diagram of low-temperature comminution and the photograph of the premix. (b) Schematic diagram of the extrusion casting process and the photograph of SPWTTP PCFF.



foaming. Due to the low hardness, low modulus, and low melting point of paraffin, it was easy to stick together, making it difficult to obtain even fine powder by directly powdering. Therefore, the liquid nitrogen was used to freeze the paraffin first and then powdered it. After crushing with a mechanical pulverizer, a finely divided paraffin powder was obtained. Then, upon mixing this paraffin powder with SEBS, EMs and ab-PP powders (the ab-PP masterbatch was also crushed into powder by the mechanical pulverizer before being mixed with the other powders), we obtained a macroscopically homogeneous premix, as shown in the upper right photograph of Fig. 1a.

The premix was extruded into sheets using an extrusion casting machine through a T-shaped die, as depicted in Fig. 1b. At high temperatures, due to the existence of the high-content paraffin, the SEBS/paraffin gel system showed a low melt strength, making the film rupture and discontinuous after coming out of the die. When the temperature dropped, SEBS/paraffin showed greater elasticity, making the material difficult to process. Therefore, the melt properties of a material play a critical role for the preparation of foaming film.

PP is a kind of general polymer material with good melting processing performance, and the addition of ab-PP masterbatch is expected to improve the processability of SEBS/paraffin. Fig. 2 compared the difference of melt properties of SPWT (without ab-PP masterbatch) and SPWTPP samples by their photos in the extrusion casting-foaming process. During these

processes, foaming was carried out simultaneously, which caused the disruption of the melt and decrease of melt strength due to the presence of pores. Fig. 2a shows the SEM micrograph of SPWT PCFF. It was observed that the expanded EMs were evenly distributed in SPWT. Their size was obviously larger than the size of the as-received EMs (Fig. S1a, ESI<sup>†</sup>), but smaller than the size of the expanded EMs in air (Fig. S1b, ESI<sup>†</sup>), which might be attributed to the restriction of the melt static pressure caused by the SEBS/paraffin/ab-PP blend. The photograph in the corner of Fig. 2a showed that the extrudate severely cracked at the extrusion casting die, resulting in a broken film as shown in Fig. 2b. This might be attributed to the low strength and high elasticity of the blend melt.

As shown in the SEM micrograph of SPWTPP in Fig. 2c, the SPWTPP was also filled with expanded EMs microspheres. Through calculation of the porosity and statistics of the microsphere diameter, it was found that SPWTPP had relatively lower porosity than SPWT, 50.8% and 45.8%, respectively (Fig. S4, ESI<sup>†</sup>), and the microsphere diameter also has a similar distribution (Fig. S5, ESI<sup>†</sup>), indicating that SPWTPP also had undergone an adequate foaming process. As shown in the photograph of SPWTPP (Fig. 2c and d), almost no cracking phenomenon was observed, and the extruded cast film showed uniform thickness and flat surface.

For this phase change foaming system, the foaming performance is determined by the melt properties of the blend system. The effect of ab-PP masterbatch addition on the melt properties was tested by rheology. Fig. 3a shows the curves of the storage modulus ( $G'$ ) and loss modulus ( $G''$ ) of the SPW and SPWPP phase change films at 180 °C as a function of frequency. It was observed that the addition of the ab-PP masterbatch significantly increased both  $G'$  and  $G''$  (a schematic diagram to illustrate the film structure at high temperature and usual temperature can be found in Fig. S6, ESI<sup>†</sup>). Fig. 3b shows the viscosity change curve of the SPW and SPWPP phase change films during the above rheological test. Both viscosities decreased with increasing frequency, which was attributed to the shear-thinning properties of the polymers. Notably, the viscosity of SPWPP was always higher than that of SPW in the entire frequency range investigated, and the slope of the viscosity change curve of SPWPP was larger. This observation revealed that the shear-thinning trend of SPWPP was more significant, indicating that the addition of the ab-PP masterbatch effectively improved the melt processability of the material, thereby obtaining smooth and flat PCFF.

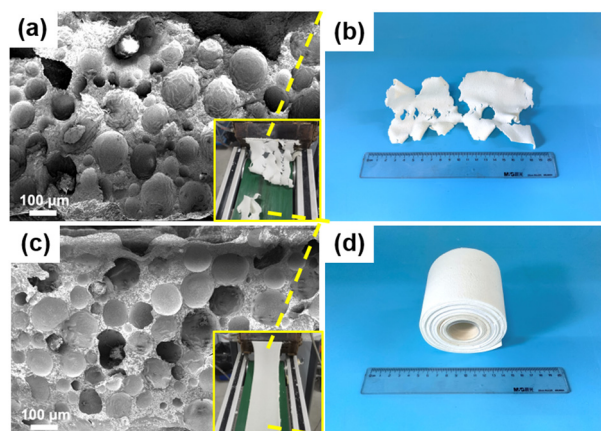


Fig. 2 (a) A SEM micrograph and (b) a photograph of SPWT PCFF. (c) A SEM micrograph and (d) a photograph of SPWTPP PCFF.

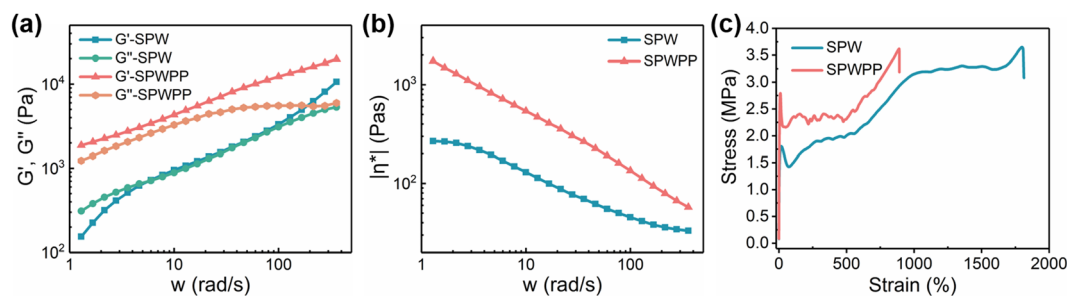


Fig. 3 (a)  $G'$  and  $G''$ , (b) viscosity and (c) stress-strain curves of SPW and SPWPP.





The mechanical properties of materials are important factors affecting their practical applications. To evaluate the tensile properties of SPW and SPWPP, the elongation at break and elastic modulus were measured, and the results are presented in Fig. 3c and Fig. S7 (ESI<sup>†</sup>), respectively. The elongation at break of SPWPP (900%) was significantly lower than that of SPW (1800%). From the perspective of elastic modulus (Fig. S7, ESI<sup>†</sup>), the elastic modulus of SPW was 38.5 MPa, while that of SPWPP was 52.1 MPa, which was attributed to the high strength of ab-PP masterbatch.

Fig. 4a displays the stress-strain curves of SPWT and SPWTTP. Obviously, compared with SPWT, the tensile strength and elongation at break of the SPWTTP PCFF increased. In addition, the elastic modulus of SPWTTP was (47.5 MPa) higher than that of SPWT (41.5 MPa), which was attributed to the high strength of PP (Fig. S8, ESI<sup>†</sup>). The above result indicated that the addition of ab-PP masterbatch improved the mechanical properties of our flexible porous phase change foaming film. High-phase change enthalpy is significantly important for the application of materials in the thermal management field. The phase change enthalpy values of the two films were measured using DSC. The melting and crystallization curves were shown in Fig. 4b, and the detailed melt and crystallization temperatures, and enthalpy values were recorded in Table 1. It could be seen that the melting enthalpy of SPWT was as high as 139.1 J g<sup>-1</sup>. After adding ab-PP masterbatch, the enthalpy of SPWTTP decreased due to a decrease in the relative content of paraffin, but the enthalpy value of SPWTTP was still at a relatively high level compared to various porous phase change materials reported in the literature,<sup>24–27</sup> measuring 128.8 J g<sup>-1</sup>. This indicated that the high phase change enthalpy of the PCFF was maintained on the basis of improved mechanical properties and melt processability.

Leakage of paraffin during the heating and cooling process would greatly affect the practical performance of the films. To assess the thermal stability of the PCFF, a leakage test was conducted. As shown in Fig. 4c<sub>1</sub>, PW sheet, SPWT, and SPWTTP PCFF of the same size were placed in a watch glass with a filter paper at the bottom, and the watch glass was placed in an oven at 80 °C (above the melting point of paraffin investigated, 52 °C). The leakage performance of each sample was observed, and their photographs at different times were recorded, as shown in Fig. 4c<sub>2</sub>–c<sub>4</sub>. During this process, it was found that the paraffin sheet melted about at 3 min (Fig. 4c<sub>2</sub>), while the SPWT and SPWTTP PCFF did not show leakage at this time. At 6 min, the paraffin had melted completely (Fig. 4c<sub>4</sub>). Throughout the entire process, SPWT and SPWTTP PCFF did not exhibit any significant leakage, indicating that they had good thermal stability, which established a foundation for their various healthcare applications.

### Heat storage and release behavior and antibacterial properties of SPWTTP PCFF

Due to the exothermic effect of paraffin in a constant temperature, the SBES/paraffin system was studied and applied as a thermotherapy material. Our previous work<sup>18</sup> proved that the heat storage and release capacity of paraffin and the thermal barrier capacity of the porous structure could achieve synergistic thermal management performance, which could effectively prolong the duration of the phase change process and achieve long-term thermotherapy effect. In this work, we also explored the exothermic properties of SPWTTP PCFF to evaluate its thermotherapy potential. The thickness of a single layer of SPWTTP PCFF was about 0.776 mm, which is too thin and might cause rapid heat release due to the relatively large contact area of the film with the environment. Here, we stacked several layers to explore their exothermic behavior. The SPWTTP PCFF with different layers (1, 2, 3, 4 and 5 layers) were heated to 80 °C in an oven, and then placed on a hot stage at 35 °C (simulating human body temperature). The hot stage was covered with a layer of cotton cloth to prevent heat exchange between the PCFF and the environment, and a thermocouple was inserted into the bottom layer of the foaming film to record the temperature change. The results were shown in Fig. 5a. It can be observed that the temperature of all SPWTTP PCFF exhibited a decreasing trend over time, and the temperature dropped sharply before reaching 48 °C (near the crystallization temperature of paraffin). This was due to the large temperature difference between SPWTTP and the hot stage, resulting in a strong heat transfer driving force between them. When the temperature dropped below 48 °C, the cooling rate slowed down significantly, which was attributed to the thermostatic exothermic performance of paraffin during the phase change process and low thermal conductivity due to the presence of a large number of pores. In the subsequent process, SPWTTP always maintained a slow exothermic rate, which might be due to the small temperature difference between SPWTTP and the hot stage, making the heat transfer driving force decrease.

Fig. 5b shows the cooling time of SPWTTP PCFF with different layers from 48 to 35 °C. It could be clearly seen that

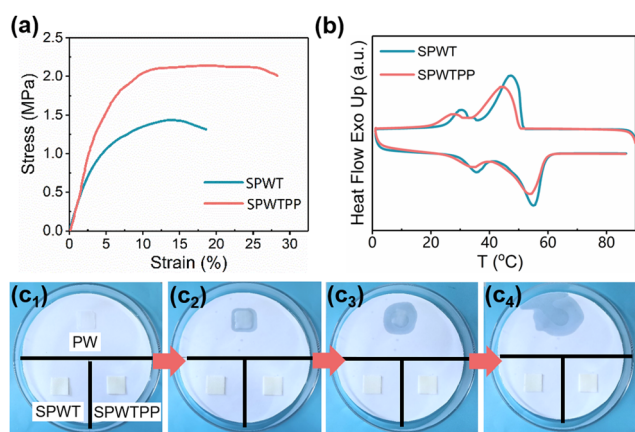


Fig. 4 (a) Stress-strain curves and (b) DSC curves of SPWT and SPWTTP. (c<sub>1</sub>–c<sub>4</sub>) Leakage of PW, SPWT and SPWTTP during heating.

Table 1 DSC characterization of SPWT and SPWTTP

Samples	Heating		Cooling	
	$T_m$ (°C)	$\Delta H_m$ (J g <sup>-1</sup> )	$T_c$ (°C)	$\Delta H_c$ (J g <sup>-1</sup> )
SPWT	55.04	139.1	47.47	137.3
SPWTTP	52.71	128.8	45.04	124.3



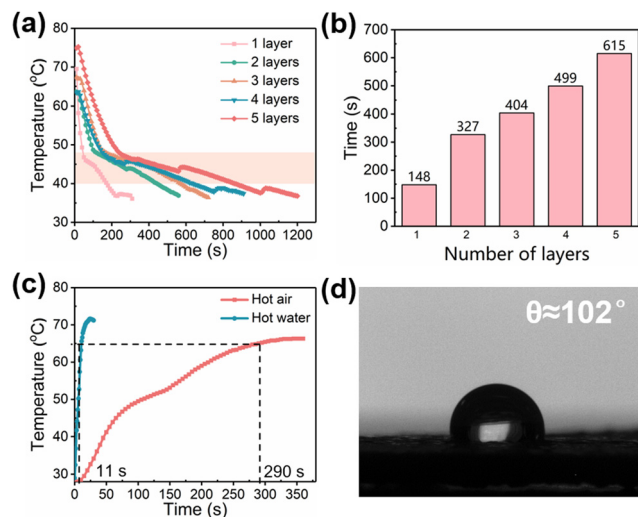


Fig. 5 (a) Temperature change curves of SPWTPP PCFF with different layers. (b) The cooling time for the above SPWTPP PCFF from 48 to 35 °C. (c) Temperature change curves of SPWTPP PCFF in hot air and hot water. (d) Contact angle of SPWTPP PCFF.

the heat release time increased with increasing PCFF layers. The reason could be attributed to two points: (1) more layers of the phase change foaming film could store more heat. (2) The superposition of multiple layers introduced a thin insulating air layer between the films, which might have further slowed down the exothermic process of paraffin. For 5-layer PCFF with a thickness of 3.7 mm and a coverage area of about 109 cm<sup>2</sup>, the total mass was only about 16.2 g but the exothermic time could be up to 10 min, indicating that the material exhibited potential as an efficient lightweight thermotherapy material.

From the exothermic performance of the SPWTPP PCFF, it showed the potential to be used as a high-efficiency thermotherapy material. Considering that the speed of heat storage was an important factor affecting the practical application of thermotherapy materials, two potential household heating methods (hot-air and hot-water methods) were explored to observe the heat storage performance of SPWTPP PCFF, and the results were shown in Fig. 5c. Obviously, the temperature

rise rate of SPWTPP in hot water was faster than that in hot air. It took about 5 minutes to rise from room temperature to 65 °C in hot air. At about 50 °C, the rate slowed down, which was due to the thermostatic endothermic performance of paraffin. In hot water, this process only took 11 s, and no obvious phase change process was observed. The contact angle test result was shown in Fig. 5d. The contact angle of SPWTPP was about 102°, which was a higher value, proving the excellent hydrophobicity of the material. Considering that the fast heating method could reduce the waiting time of the thermotherapy product users and make the treatment process more efficient, the excellent hydrophobicity of the materials and the feature of rapid heating in water made our SPWTPP PCFF very suitable for thermotherapy applications.

As a wearable product in contact with the human body, a qualified antibacterial rate was one of the necessary requirements. The antibacterial properties of SPWT and SPWTPP to *E. coli* and *S. aureus* were tested by plate coating counting method, and the results are shown in Fig. 6. Fig. 6a<sub>1</sub>–a<sub>3</sub> respectively showed the distribution of colonies in the culture solution after *E. coli* was cultured in the Petri dishes containing SPWTPP, SPWT and the standard control group. It was clear that almost no colonies could be observed in the bacterial solution containing SPWTPP PCFF, while a large number of bacteria were observed in SPWT and the standard control group. Similarly, Fig. 6b<sub>1</sub>–b<sub>3</sub> showed the antibacterial test photographs of SPWTPP, SPWT and the control group against *S. aureus*. Only the bacteria solution containing SPWTPP PCFF did not exhibit the bacteria, indicating that SPWTPP had an excellent antibacterial effect. The antibacterial rates of SPWTPP and SPWT against the two bacteria were calculated by the number of colonies in the photographs, and the results were shown in Fig. 6c. SPWTPP showed an antibacterial rate of up to 100% against *E. coli* and *S. aureus*, which laid the foundation for the application of SPWTPP PCFF as the wearable thermotherapy device.

#### Thermotherapy performance demonstration of SPWTPP PCFF

The characteristics of fast heat charge and slow heat release of SPWTPP PCFF makes it an ideal material for the thermotherapy application. As shown in the corner of Fig. 7a–c, The SPWTPP phase change foaming film was used as the inner layer of shoulder pads, eyeshades, and masks. Fig. 7a–c showed the infrared images

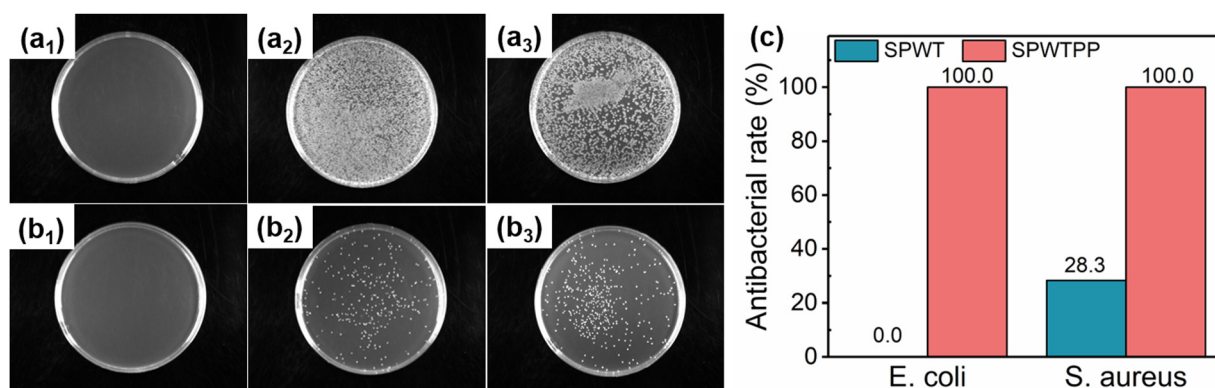


Fig. 6 Antibacterial test photographs of SPWTPP, SPWT and the standard control group against (a<sub>1</sub>)–(a<sub>3</sub>) *E. coli* and (b<sub>1</sub>)–(b<sub>3</sub>) *S. aureus*. (c) Calculated antibacterial rate of SPWTPP and SPWT against *E. coli* and *S. aureus*.

of these thermotherapy products heated to 60 °C and used for thermotherapy on the shoulder, eyes and mouth, respectively. In this process, the heat stored in the paraffin of SPWTTP was released slowly due to the thermal barrier of pores. When the heat release rate slowed down near the phase change temperature of paraffin, the heat was released more slowly due to the thermostatic exothermic effect of paraffin. This helped maintain a comfortable thermotherapy temperature of around 45 °C for a longer period of time, contributing to a longer-duration thermotherapy effect.

The SPWTTP PCFF can also be utilized to make knee protector for treating arthritis-related diseases, as shown in Fig. 7d. The knee protector, after being heated to 60 °C, was placed on the user's knee and fixed, while the temperature of the SPWTTP at the contact position with the human body was recorded with a thermocouple. The temperature change curve of SPWTTP PCFF in thermotherapy application for the knee was recorded, as shown in Fig. 7e. Considering the phase change temperature of paraffin and the comfortable temperature range for thermotherapy, the heat release duration of SPWTTP PCFF in the range of 40–52 °C was finally recorded. Before 52 °C, the temperature of SPWTTP decreased rapidly, which was attributed to the large temperature difference between SPWTTP and the environment. When approaching the phase change temperature of paraffin, the temperature decreased slowly, which was due to the thermostatic exothermic effect and the reduced temperature difference between SPWTTP and the human body. The duration for SPWTTP PCFF of dropping from 52 to 40 °C was about 25 min. According to literature reports,<sup>14,28</sup> a single thermotherapy for more than 20 min could achieve a satisfying therapeutic effect for some diseases such as allergic rhinitis and arthritis, which indicated that SPWTTP could completely satisfy the requirement of thermotherapy in the medical treatment field.

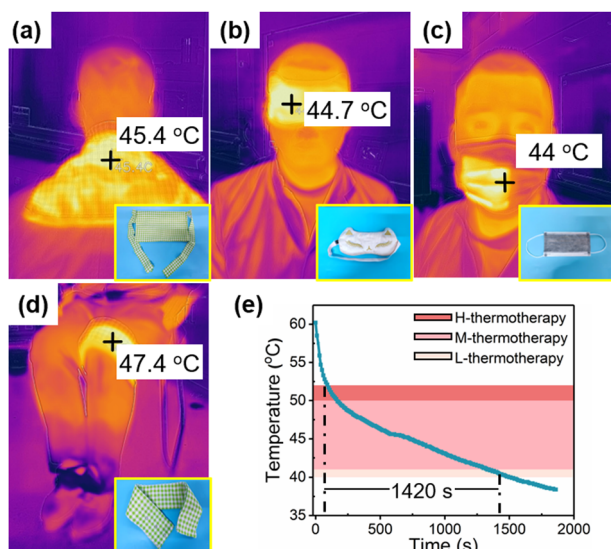


Fig. 7 Infrared images and photographs of SPWTTP PCFF, which were prepared in the (a) thermotherapy shoulder protector, (b) thermotherapy eyeshade, (c) thermotherapy mask, and (d) thermotherapy knee protector. (e) Temperature change curve during the thermotherapy of the SPWTTP knee protector.

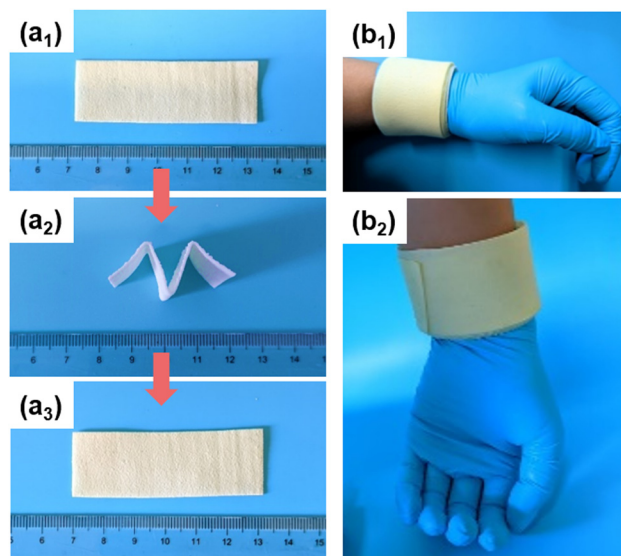


Fig. 8 Photographs of the SPWTTP film (a<sub>1</sub>) in the original shape, (a<sub>2</sub>) programmed into the "M" shape at 65 °C and then cooled down to room temperature, (a<sub>3</sub>) heated again to 65 °C, (b<sub>1</sub>) wrapped around the wrist in 5 layers and (b<sub>2</sub>) when the wrist was placed vertically.

The SEBS/paraffin system, which contained a crystallizable fixing phase (paraffin) and an elastic recovering phase (SEBS), was a kind of interesting shape memory material.<sup>29–33</sup> Utilizing the shape memory properties of the material, it could be used as a wearable device that could be firmly attached to various parts of the human body. Here, the shape memory properties of the SPWTTP phase change foaming film were tested, and the results are shown in Fig. 8a<sub>1</sub>–a<sub>3</sub>. A piece cut from SPWTTP PCFF (Fig. 8a<sub>1</sub>) was heated to about 65 °C in hot water, and folded into the shape of "M" at this temperature. The shape was fixed after cooling to room temperature, as shown in Fig. 8a<sub>2</sub>. When the temperature of the SPWTTP PCFF was raised to 65 °C again, its shape was completely restored, as shown in Fig. 8a<sub>3</sub>, and no obvious creases were observed, indicating that the material had good shape memory properties. The characteristics were expected to help the material adhere to various parts of the human body in practical applications to achieve better thermotherapy effects.

We also tested how well the SPWTTP PCFF held on to the wrist, and the result is shown in Fig. 8b<sub>1</sub> and b<sub>2</sub>. Using the characteristics of shape memory, the SPWTTP PCFF was heated up and wrapped around the wrist while it was hot. After cooling, it could be seen that each layer of the SPWTTP PCFF was tightly attached to the wrist (Fig. 8b<sub>1</sub>). When the wrist was put vertically, as shown in Fig. 8b<sub>2</sub>, no obvious slipping was observed under the action of gravity, indicating that the PCFF had good flexibility and could be fit well with the human joints due to the shape memory performance, which allowed the user to move around freely during the treatment process.

## Conclusions

In summary, a flexible SEBS/paraffin based porous phase change foaming film was successfully prepared through a one-step melt





extrusion casting-foaming technology. By low-temperature crushing of paraffin and blending with ab-PP masterbatch, the challenge of the simultaneous continuous extrusion and foaming of the phase change composites with high-content paraffin was overcome, obtaining a PCFF with a phase change enthalpy of up to  $128.8 \text{ J g}^{-1}$  and a porosity of 45.8%. The high phase change enthalpy and existence of abundant pores enabled the resulting film with longer heat release duration. The heat release results of SPWTPP showed that the 5-layer SPWTPP PCFF could maintain heat release for up to 10 min, and it only took 11 s to charge in hot water, exhibiting the characteristics of fast charge and slow heat release. SPWTPP PCFF also possessed good flexibility and shape memory, making it easy to be combined with textiles to prepare various thermotherapy products such as shoulder pads, eyeshades, masks, and knee pads, which could be firmly attached to human body parts during use. The SPWTPP phase change foaming film could maintain the thermotherapy effect for about 25 min, which totally satisfied the requirement of thermotherapy for some diseases such as allergic rhinitis, arthritis. Furthermore, the ab-PP endowed the material with excellent antibacterial properties, which showed an antibacterial rate of up to 100% against both *E. coli* and *S. aureus*, indicating its potential as wearable thermotherapy products. Overall, this study provides a new and promising direction for the development of PCFF in the field of thermotherapy and healthcare.

## Conflicts of interest

There are no conflicts to declare.

## Acknowledgements

We gratefully acknowledge the financial support from the National Natural Science Foundation of China (no. 52173056 and 51773040). The authors sincerely appreciate Professor Yong Guan from East China University of Science and Technology for the helpful discussion on antibacterial masterbatch application.

## Notes and references

- 1 S. Zhu, C. W. Lou, S. Zhang, N. Wang, J. Li, Y. Feng, R. He, C. Xu and J.-H. Lin, *Surf. Interfaces*, 2022, **29**, 101689.
- 2 B. Gu, X. Huang, F. Qiu, D. Yang and T. Zhang, *ACS Sustainable Chem. Eng.*, 2020, **8**, 15936–15945.
- 3 Y. Chen, B. Zhao, H. Zhang, T. Zhang, D. Yang and F. Qiu, *Chem. Eng. J.*, 2022, **450**, 138177.
- 4 J. Xie, Y. Zhang, J. Dai, Z. Xie, J. Xue, K. Dai, F. Zhang, D. Liu, J. Cheng, F. Kang, B. Li, Y. Zhao, L. Lin and Q. Zheng, *Small*, 2023, **19**, e2205853.
- 5 Y. Zhang, L. Wang, B. Tang, R. Lu and S. Zhang, *Appl. Energy*, 2016, **184**, 241–246.
- 6 R. Gulfam, P. Zhang and Z. Meng, *Appl. Energy*, 2019, **238**, 582–611.
- 7 L. Liu, X. Shan, X. Hu, W. Lv and J. Wang, *ACS Nano*, 2021, **15**, 19771–19782.
- 8 C. Jia, X. Geng, F. Liu and Y. Gao, *Case Stud. Therm. Eng.*, 2021, **25**, 100938.
- 9 A. Tinti, A. Tarzia, A. Passaro and R. Angiuli, *Appl. Therm. Eng.*, 2014, **70**, 201–210.
- 10 Y. Qu, J. Chen, L. Liu, T. Xu, H. Wu and X. Zhou, *Renew. Energy*, 2020, **150**, 1127–1135.
- 11 P. Liu, H. Gao, X. Chen, D. Chen, J. Lv, M. Han, P. Cheng and G. Wang, *Composites, Part B*, 2020, **195**, 108072.
- 12 M. Li, Z. Qin, Y. Cui, C. Yang, C. Deng, Y. Wang, J. S. Kang, H. Xia and Y. Hu, *Adv. Mater. Interfaces*, 2019, **6**, 1900314.
- 13 S. Song, H. Ai, W. Zhu, L. Lv, R. Feng and L. Dong, *Composites, Part B*, 2021, **226**, 109330.
- 14 X. Chen, H. Gao, G. Hai, D. Jia, L. Xing, S. Chen, P. Cheng, M. Han, W. Dong and G. Wang, *Energy Storage Mater.*, 2020, **26**, 129–137.
- 15 J. H. Jing, H. Y. Wu, Y. W. Shao, X. D. Qi, J. H. Yang and Y. Wang, *ACS Appl. Mater. Interfaces*, 2019, **11**, 19252–19259.
- 16 W. Aftab, A. Mahmood, W. Guo, M. Yousaf, H. Tabassum, X. Huang, Z. Liang, A. Cao and R. Zou, *Energy Storage Mater.*, 2019, **20**, 401–409.
- 17 P. Sobolciak, M. Mrlik, A. Popelka, A. Minarik, M. Ilcikova, P. Srnc, Z. Nogellova, M. Ouederni and I. Krupa, *Polymers*, 2021, **13**, 1987.
- 18 X. Guo and J. Feng, *Composites, Part B*, 2022, **245**, 110203.
- 19 F. Seidi, M. Khodadadi Yazdi, M. Jouyandeh, M. Dominic, H. Naeim, M. N. Nezhad, B. Bagheri, S. Habibzadeh, P. Zarrintaj, M. R. Saeb and M. Mozafari, *Int. J. Biol. Macromol.*, 2021, **183**, 1818–1850.
- 20 D. Wei, Y. Ding, T. Wang, J. Yang, Y. Guan and A. Zheng, *J. Appl. Polym. Sci.*, 2017, **134**, 44190.
- 21 W. Cao, D. Wei, A. Zheng and Y. Guan, *Eur. Polym. J.*, 2019, **118**, 231–238.
- 22 P. Sengupta and J. W. M. Noordermeer, *J. Elastomers Plast.*, 2016, **36**, 307–331.
- 23 D. Tomacheski, M. Pittol, C. E. Ermel, D. N. Simões, V. F. Ribeiro and R. M. C. Santana, *Polym. Bull.*, 2017, **74**, 4841–4855.
- 24 M. You, X. Zhang, J. Wang and X. Wang, *J. Mater. Sci.*, 2009, **44**, 3141–3147.
- 25 M. You, X.-x Zhang, X.-c Wang, L. Zhang and W. Wen, *Thermochim. Acta*, 2010, **500**, 69–75.
- 26 X. Li, H. Chen, H. Li, L. Liu, Z. Lu, T. Zhang and W. H. Duan, *Appl. Energy*, 2015, **159**, 601–609.
- 27 M. Song, J. Jiang, J. Zhu, Y. Zheng, Z. Yu, X. Ren and F. Jiang, *Carbohydr. Polym.*, 2021, **272**, 118460.
- 28 Q. Zhang, Z. He, X. Fang, X. Zhang and Z. Zhang, *Energy Storage Mater.*, 2017, **6**, 36–45.
- 29 S. Song, J. Feng and P. Wu, *Macromol. Rapid Commun.*, 2011, **32**, 1569–1575.
- 30 Q. Zhang, Y. Zhao and J. Feng, *Sol. Energy Mater. Sol. Cells*, 2013, **118**, 54–60.
- 31 S. Ren and J. Feng, *Adv. Mater. Technol.*, 2022, **7**, 2200339.
- 32 S. Zhao and J. Feng, *Chinese J. Polym. Sci.*, 2022, **40**, 1697–1705.
- 33 S. Ren and J. Feng, *Adv. Mater. Technol.*, 2023, **8**, 2300029.

